UMM-7

Copy No. 54

UNIVERSITY OF MICHIGAN

Ann Arbor

EXTERNAL MEMORANDUM NO. 7

Project MX-794
(AAF Contract W33-038 ac-14222)

Project "Wizard"

"A Simplified Method of Calculating Ram-Jet Performance Applicable To High Mach Numbers"

Prepared by James R. Gannett
James R. Gannett

Approved by E. T. Vincent
E. T. Vincent
Professor of Mechanical Engineering

July 23, 1947

ACKNOWLEDGEMENT

The author wishes to express sincere appreciation for the assistance given by Mr. John R. Sellars, whose suggestions and knowledge of the relationships previously developed and used herein have been most valuable.

CONTENTS

Page

Introduction 1

Summary 2

Conclusions 4

List of Symbols 6

Discussion 8

Combustion Chamber 10

Exit Nozzle 22

Thrust Coefficient 26

Diffuser 27

Brief Outline of Method 30

Sample Calculation I 32

Sample Calculation II 35

Sample Calculation III 37

References 39

Appendix I 40

Appendix II 43

LIST OF ILLUSTRATIONS

Figure	Title	Page
A	Ram-Jet Station Designation.	46
1	Solution for Velocity at Station 3 (Ram-Jet)	47
1A	Solution for V_3 (Ram-Jet).	48
2	Chart for Use in Calculating A_1/A_2	49
2A	Total Temperature vs. Flight Mach Number . .	50
2B	Diffuser Efficiency vs. Mach Number	51
3	Specific Stream Thrust - $\frac{F_2}{W_a}$ vs. T_2 for Various V_2's.	52
3A	Heat Release - S_a vs. T_2	53
3B	S_a vs. T_2.	54
3C	S_a vs. T_2.	55
3D	S_a vs. T_2.	56
3E	S_a vs. Fuel-Air Ratio.	57
4	$\phi(M)$ vs. Mach Number	58
4A	$\phi(M)$ vs. Mach Number	59
4B	$\phi(M)$ vs. Mach Number	60
5	$\phi(M)$ vs A/A_t	61
5A	Theoretical Total Pressure Recovery for a Constant Nozzle Efficiency Based on Energy.	62
6	Maximum V_2 for $A_1 = A_2$ and Various Fuel-Air Ratios.	63
7	Thrust Coefficient vs. Flight Mach Number.	64

INTRODUCTION

The propulsion problems related to Project MX-794, (Project Wizard) initially drew attention to the ram-jet as a possible propulsion unit and performance estimates for various flight conditions were desired. A brief survey of the then existing methods of calculating ram-jet performance revealed that there were almost as many methods as there were groups investigating the ram-jet. Most of the methods were purposely developed holding constant certain important variables such as fuel-air ratio, various efficiency curves, temperatures at the end of the combustion chamber, or general configuation, thus lacking the latitude of applications desired of a general method of calculation. Furthermore, Project Wizard is concerned with a wide range of Mach numbers (2-6) and the methods then in general use incorporated certain assumptions which are not valid at high Mach numbers. As a result, a method was devised (see Ref. 6) which is valid at high Mach numbers of flight, has the generality desired and is believed to give accurate results. However, this method is quite lengthy and tedious, and does not make readily apparent the important variables affecting performance. Certain subsequent investigations by Project Wizard using this method and the knowledge of some relationships previously developed by another group (see Ref. 3, 4, 5) led to the development of the simplified method presented in this report.

SUMMARY

The method developed in this report permits rapid calculation of ram-jet performance and still incorporates in a satisfactory manner the major effects of molecular dissociation in the combustion process and the variable specific heats of air as well as of the products of combustion. Variables such as the diffuser, combustion, and nozzle efficiencies; and operating factors, such as the velocity of the air at the entrance to the combustion chamber and the fuel-air ratio, can be assigned any value considered practical for the purpose at hand. The general configuration of the ram-jet can be varied as desired and the temperature at the combustion chamber exit can be selected, or allowed to assume whatever magnitude it will, depending on the particular conditions.

The maximum possible velocity at the combustion chamber entrance determined by the fundamental equations of flow (that entrance velocity which produces sonic velocity or "choking" at the combustion chamber exit) is easily found for any Mach number, altitude, and fuel-air ratio. Also, at low Mach numbers of flight the existence of two solutions for the equations governing flow in the ram-jet combustion chamber is recognized and explained by the graphs and equations presented herein.

Included in the last pages of this report is a condensed outline of the method, with three typical calcu-

lations, each representing a common problem. Appendix I presents a discussion of the method for calculating ramjet performance as given in Reference 6 regarding its application to the condition where "choking" is present at the combustion chamber exit; and Appendix II is a discussion pertaining to the magnitude of the velocity at the combustion chamber entrance as determined by design considerations and the "choking" condition.

CONCLUSIONS

1. The upper limit on the air velocity at the combustion chamber entrance, V_2, for high Mach numbers of flight, imposed by the fundamental equations governing flow in a duct, is well above the velocities at which it is possible to sustain combustion at the present time, regardless of fuel-air ratio. Therefore, for flight at high Mach numbers, high velocities at the combustion chamber entrance are theoretically possible if "blow-out" and other practical difficulties can be overcome.

However, since studies of the variation of the thrust coefficient, C_t, with changes in general ram-jet configuration at high Mach numbers of flight indicate that maximum C_t is obtained when the cross-sectional area of the diffuser inlet equals that of the combustion chamber; and, because at lower Mach numbers of flight, V_2 is limited by the "choking" condition at the combustion chamber exit, it is not expected that combustion chamber entrance velocities over 500 ft per sec will be practical except in very special instances.

2. The stagnation temperature after combustion and the flow velocity at the combustion chamber entrance appear as important variables affecting ram-jet performance.

3. The variation of the specific heats and the degree of molecular dissociation with temperature is appreciable under the conditions encountered in a ram-jet at Mach

numbers of flight greater than 2 with fuel-air ratios which give maximum thrust and can be accounted for in a simple manner as shown in this report. The variation of the above effects due to different pressures at given temperatures can not be accounted for without use of the Thermodynamic Charts (see Reference 2) and their accompanying lengthy calculations, but the variation is negligibly small compared with that due to temperature.

LIST OF SYMBOLS

A = area - sq ft

a = acceleration - ft per sec per sec

C = velocity of sound - ft per sec

C_t = thrust coefficient

C_s = velocity of sound at stagnation temperature - ft per sec

F = stream thrust - lb

$\frac{F}{W_a}$ = specific stream thrust - sec

f = weight of fuel - lb

g = gravitational acceleration - ft per sec per sec

γ = ratio of specific heats $(\frac{c_p}{c_v})$

h = enthalpy - Btu per lb

h_{2P} = fictitious enthalpy used to relate pressures in a non-isentropic adiabatic process

h_{2V} = actual enthalpy, assuming no losses through wall boundaries

J = conversion factor, 778 ft lb = 1 Btu

M = Mach number

m_f = mass flow - slugs per sec

η_c = combustion efficiency based on heating value of fuel

η_D = diffuser efficiency based on energy considerations

η_n = nozzle efficiency based on energy considerations

η_{np} = nozzle efficiency based on total pressure considerations

η_p = diffuser efficiency based on pressure recovery

η_{S_a} = combustion efficiency based on 100 %S_a

P = pressure - lbs per unit area

Pr = pressure ratio (adiabatic processes - see Reference 1)

R = gas constant - 53.345 ft lb per lb per ^{o}R

S_a = function of total temperature - sec

T = static temperature - ^{o}R

T_g = gross thrust - lb

T_t = total temperature - ^{o}R

V = flow velocity - ft per sec

W_a = weight flow of air - lb per sec

ρ = density - lb per cu ft

Subscripts:

1, 2, 2', 3, 4, and 5 refer to stations (see Figure A)

DISCUSSION

A method for calculating ram-jet performance at high Mach numbers was presented in Reference 6. It successfully accounts for molecular dissociation and variable specific heats, both of which have an appreciable effect on performance at high velocities of flight with the fuel-air ratios used (.0605, .0665 and .0782 by weight). Although the method presented in Reference 6 is quite lengthy and tedious, it is believed that the results obtained by its use will be accurate within the efficiency assumptions, calculation error, and chart (Reference 2) accuracy, in accounting for variable specific heats and dissociation in the burning and expansion process. Thus the accuracy of any other simplified method may be evaluated with reference to the results obtained therefrom.

It is known that the conditions at the entrance to the combustion chamber and the amount of fuel added can uniquely determine the conditions after combustion. It remains to express this relationship in a simple manner which will still account for the effects of dissociation, variable specific heats, etc. Such a simplification would eliminate the use of the Thermodynamic Charts (Reference 2) and their attending complicated calculations. Therefore, if variable specific heats and dissociation in the combustion process are to be accounted for, which appears necessary at high Mach numbers, this relationship between the properties of the gases at stations 2 and 3 (see

Figure A) must in some manner incorporate previous calculations which have made use of either the Thermodynamic Charts or an equivalent method. Also the relationship should show the presence of two solutions at station 3 (one subsonic, one supersonic) at low Mach numbers and the reason for disappearance of the supersonic solution at higher Mach numbers, as discussed in Appendix I.

An analysis of flow through a ram-jet has been made by a group at JHU/APL, Silver Spring, Md. (References 3, 4, 5) where it was shown to be possible to express the conditions after burning as a function of conditions before burning and heat added. Their analysis as presented in these reports is believed accurate for low flight Mach numbers (< 2) but is not adaptable to higher flight Mach numbers without revision, for the following reasons: investigations at the University of Michigan have shown that at Mach numbers greater than approximately 2.75, performance is impaired by the lack of a tail nozzle (the configuration used by the APL investigators); and the calculation of conditions through the diffuser by use of Mach number relationships based on constant specific heats is sufficiently accurate at Mach numbers less than 2, but at higher Mach numbers neither of the above are recommended if maximum performance and accurate results are desired. For instance, if one were to use the Mach number relations in calculating total temperature or the temperature after the diffuser at a flight Mach number of 6 at sea level, $4260^{\circ}R$ would be the result if a specific heat ratio (γ) of

1.4 were used, and 2390°R if a γ of 1.2 were used. Thus the variation of γ over this possible range (1.4-1.2) is quite critical in such a calculation and the task of choosing the correct mean value is essentially one of trial and error. By using the Air Tables (Reference 1), as outlined in Reference 6, where the varying specific heats are accounted for, the temperature for the above conditions is found to be 3749°R.

It is also generally known that a tail nozzle is a necessary item on the ram-jet at high Mach numbers, especially since its addition makes a considerable contribution to the thrust coefficient. The necessity of a tail nozzle at high Mach numbers of flight arises from the fact that the velocity at the entrance to the combustion chamber would be excessive, accompanied by lowered pressure, if no nozzle were employed (mass flow constant for a given set of flight conditions), thus causing poor combustion efficiency and, probably, "blow-out". Also, for a ram-jet of given configuration, the lowest V_2 possible without causing a spillover is desirable, because the thrust per unit mass flow in the duct decreases with an increase in V_2. Thus the remainder of this report is an extension of the relationships already known to higher Mach numbers, with a development that permits a clear understanding of the important functions.

Combustion Chamber

In developing the relationship between stations 2 and 3 the following assumptions are made:

1. A cylindrical combustion chamber is employed; i.e., constant area burning.
2. No heat losses occur through the duct walls.
3. Heating value of fuel is constant, 19,500 Btu per lb fuel ($CH_{2.25_x}$)
4. Use of the arithmetical mean of specific heats in calculations between any two temperature limits sufficiently approximates the results obtained by the exact method for an adiabatic compression or expansion.
5. No frictional losses in the combustion chamber.

See page 6 for list of symbols.

The force-momentum equation makes it possible to express conditions at station 3 as a function of those at station 2 and the heat added, viz.-

(1) $$A_2\left(P_2 + \frac{\rho_2}{g} V_2^2\right) = A_3\left(P_3 + \frac{\rho_3}{g} V_3^2\right)$$

where $$\frac{\rho}{g} VA = \frac{W_o}{g} = m_f = \text{mass flow in slugs per sec}$$

The difference in the magnitude of expression (1) between two points in a duct can be shown to represent the net force on the duct when integrated over the interior surface as shown below.

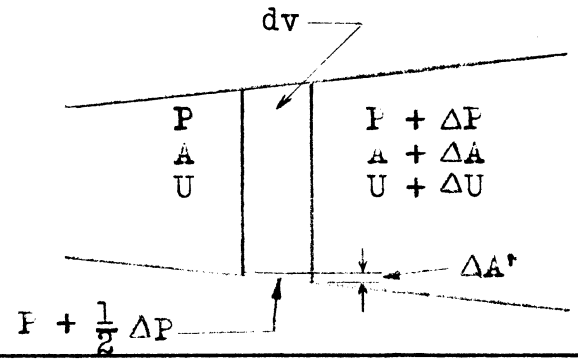

Consider a small element or region of the duct, dv. The force-momentum relation states that the net force exerted on the region is equal to the net out-flow of momentum per sec

$$\text{Force} = m_f \Delta u$$

where m_f is the mass flow undergoing the momentum change. Equating the forces acting on the region, dv, to the change of momentum of the mass flow,

$$PA - (P + dP)(A + dA) + (P + \frac{dP}{2})\, dA' = -m_f u + m_f(u + du) = + m_f\, du$$

Neglecting the products $\frac{dP}{2}\, dA'$ and dPdA and noting that PdA' is the reaction force on the wall, the integral of which is the thrust on the body,

$$PA - PA - PdA - AdP + PdA' = m_f\, du$$

$$PdA' = m_f\, du + PdA + AdP$$

The total force on the duct from station 1 to 2 then becomes:

$$\text{Force (lbs)} = \int_1^2 PdA' = m_f u + PA \Big]_1^2 = F_2 - F_1$$

Letting u = V, F represents the expression $m_f V + PA$ at any point and has been termed "stream thrust".

$$\text{Force} = F_2 - F_1 = m_{f2} V_2 + P_2 A_2 - (m_{f1} V_1 + P_1 A_1)$$

$$= A_2 \left(P_2 + \frac{\rho_2}{g} V_2^2\right) - A_1\left(P_1 + \frac{\rho_1}{g} V_1^2\right) \text{ lbs}$$

Note that the expression

$$F = A \left[P + \frac{\rho}{g} V^2\right]$$

must be a constant from station 2 to 3 in the ram-jet, that is, any cylindrical section, since $dA' = 0$ and thus

$$\int_2^3 P dA' = 0 \quad \text{i.e., } F_2 = F_3$$

Actually there is some loss of stream thrust, F, at the flame holders, which can be expressed as

$$F_2 - \text{loss at } 2' = F_3 = F_{2'}.$$

Continuity of mass flow can be written as follows, using $\frac{P}{\rho} = RT$ and $C^2 = \gamma RTg$;

$$W = \rho VA.$$

$$= \frac{\rho Vg\gamma RTA}{C^2}$$

$$W = \frac{PM\gamma Ag}{C} \tag{2}$$

Then, solving for PA and using the subscript o for ambient conditions:

$$P_o A_o = \frac{W_o C_o}{M_o \gamma_o g} \tag{3}$$

Also from the conservation of energy and the state equations,

(4) $$C_o = \frac{C_{so}}{\left[1 + \frac{\gamma-1}{2} M_o^2\right]^{\frac{1}{2}}}$$ where C_{so} is the velocity of sound at the stagnation temperature.

From (3) and (4)

(5) $$P_o A_o = \frac{W_o C_{so}}{\left[1 + \frac{\gamma-1}{2} M_o^2\right]^{\frac{1}{2}}} \frac{1}{M_o \gamma_o g}$$

also noting that

(6) $$A_o\left(P_o + \frac{\rho_o}{g} V_o^2\right) = A_o P_o (1 + \gamma M_o^2) = F_o$$

The following can be written from (5) and (6)

(7) $$F_o = \frac{W_o C_{so}}{\left[1 + \frac{\gamma-1}{2} M_o^2\right]^{\frac{1}{2}}} \frac{1 + \gamma M_o^2}{M_o \gamma g}$$

Writing F in lbs per lb of air per sec for station 3, rearranging, and multiplying by $\frac{\sqrt{2(\gamma+1)}}{\sqrt{2(\gamma+1)}}$ for a reason explained later, also noting that at station 3 the flow is (1 + f) lb of gas per lb of air, - the following is obtained

(8) $$\frac{F_3}{W_a} = \frac{C_{s3}\sqrt{2(\gamma+1)}\ (1+f)}{\gamma g} \frac{1 + \gamma M_3^2}{M_3\sqrt{2(\gamma+1)}\left[1 + \frac{\gamma-1}{2} M_3^2\right]^{\frac{1}{2}}}$$

Thus the following relationships are defined -

(9) $$S_a \equiv \frac{C_{s3}\sqrt{2(\gamma+1)}\ (1+f)}{\gamma g}$$

and the Mach number function

(9A) $$\phi(M) = \frac{1 + \gamma M^2}{M\sqrt{2(\gamma+1)}\left[1 + \frac{\gamma-1}{2}M^2\right]^{\frac{1}{2}}}$$

(multiplying by $\frac{\sqrt{2(\gamma+1)}}{\sqrt{2(\gamma+1)}}$ serves to normalize the Mach number function so that $\phi(M) = 1$ when $M = 1$). Then

(10) $$\frac{F_3}{W_a} = S_a\,\phi(M_3) \text{ lb per lb air per sec}$$

Figures 4 and 4A show $\phi(M)$ vs Mach munber for three values of γ, two of which correspond to the extreme limits of temperature to be expected at station 3. The displacement of these curves due to the maximum variation in γ is appreciable but the actual effect on the performance calculation can not yet be evaluated as these curves are used only indirectly in calculating the thrust coefficient, C_t. Figures 4 and 4A are included in the report however so that M_3 can be readily determined if desired.

Figure 4B shows that for low values of $\phi(M)$, ($\phi(M) = 1$ to $\phi(M) \approx 1.7$), there are two solutions for the Mach number at station 3, one subsonic, one supersonic. Only the subsonic solution is of practical interest, the supersonic solution being physically impossible. The supersonic solution disappears at values of $\phi(M)$ greater than approximately 1.7, as indicated above. It can be easily shown that $\phi(M)$ approaches the limit $\frac{\gamma}{\sqrt{\gamma^2 - 1}}$ for high Mach numbers. This limit is equal approximately to 1.67 and 1.91 for $\gamma = 1.25$ and 1.175 respectively. Then for $\phi(M)$ greater than approximately 1.9 only one solution for the

combustion chamber exit velocity is possible, the supersonic solution having disappeared.*

In setting up the curves for fuel-air ratios .0605, .0665 and .0782, M_3 (and thus $\phi(M_3)$ from Figure 4A) was

---

*This is, after all, exactly what one would expect as the equation relating Mach numbers before and after a normal shock,

$$M_2^2 = \frac{1 - \frac{\gamma-1}{\gamma-1}(M_1^2 - 1)}{1 + \frac{2\gamma}{\gamma-1}(M_1^2 - 1)}$$

where M_1 = the Mach number before shock, is derived from the same basic considerations, and it shows that for an increasing supersonic Mach number before shock there is a lower limit on the resulting subsonic Mach number after shock. So, conversely, one would reason that for certain subsonic Mach numbers there co-exist supersonic Mach numbers which would also satisfy the energy, force-momentum, and continuity equations even though they are of no practical significance for these flow conditions. The supersonic Mach number increases without bound as the subsonic Mach number decreases to the lower value, $\sqrt{\frac{\gamma-1}{2\gamma}}$, (let M_1 become infinite in above equation and evaluate) below which the subsonic Mach number has no co-existent supersonic Mach number. This lower subsonic value for which the supersonic Mach number disappears is approximately $M = .37$ for $\gamma = 1.4$; and can be obtained by either the $\phi(M)$ equation (Mach number corresponding to $\phi(M) = \frac{\gamma}{\sqrt{\gamma^2 - 1}}$ or the Mach number relation across a normal shock. Thus the existence of the two types of solutions given in Figures 1 and 1a and discussed in Appendix I is verified and explained.

calculated using the method given in Reference 6, which makes use of Thermodynamic charts.

The curves shown for fuel-air ratios .0499, .0333 and .01995 were obtained from calculations performed with the aid of Reference 7. The chart in Reference 7 does not account for molecular dissociation as the effect is unimportant at the lower temperatures encountered with the reduced fuel-air ratios. Because $F_{2'} = F_3$, S_a can be found from $S_a = \frac{F_{2'}}{\phi(M_3)W_a}$. Thus the important effects of dissociation and variable specific heats in the combustion process are retained and accounted for in the magnitude of S_a when found in this manner. From Equation 9, it can be seen that S_a is dependent only on total temperature at station 3. Thus, at a given combustion chamber inlet condition, T_{t2}, S_a is a function of the amount of heat added and has been termed the "heat release" or the "specific air impulse" by some investigators.

The temperature at station 3 can be calculated from the following equation which is obtained by solving for T_3 in equation (9).

$$T_3 = \frac{\gamma_3 g S_a^2}{2R(1+f)^2(\gamma+1)(1 + \frac{\gamma-1}{2} M_3^2)}$$

From this it can be seen that a constant S_a would keep T_3 approximately constant, suggesting a convenient method of calculating performance at a constant combustion chamber exit temperature. For more accurate calculations, variation in M_3 should be considered.

The effect which a large variation of pressure (60-5000 psi) at station 3 has on S_a was investigated and seems to be quite small, almost insignificant as far as the results are concerned, but is large enough to warrant an explanation. As pressure is varied, keeping the temperature at station 2 and heat added constant, the position on the Thermodynamic chart of Reference 2 representing the state of the gas after combustion moves horizontally. As can be seen on the charts, the constant temperature lines are not independent of the pressure. The slope changes slightly as pressure varies, the main cause being the varying degrees of molecular dissociation at the same enthalpies and different pressures. The method as outlined does not account for this variation due to pressure, hence there is no change in C_t for different pressures with temperature constant at station 2. Therefore, for changes in altitude at altitudes where the temperature gradient is zero (above 35,332 - NACA Standard Air) there is no change in C_t at a constant Mach number, whereas, by the method presented in Reference 6, there is a slight increase in C_t above 40,000 ft due to the change in pressure. As previously stated, the variation of $\phi(M_3)$, and thus S_a due to the effects mentioned above, was investigated over a range of pressures up to 5000 psi and found to be approximately 3 %. However, the error that does arise in the practical example is negligible.

As stated before, S_a is a function of the total temper-

ature at station 3 and therefore it can also be said that it is a function of total temperature at station 2 with a given heat addition. S_a was plotted against the total temperature at station 2 for different fuel-air ratios (see Figures 3A, 3B, 3C, 3D, and 3E). These curves are convenient, as the total temperature at station 2 is a function only of Mach number of flight and altitude, and thus easily determined (see Figure 2A). S_a has been plotted for six fuel-air ratios, however, the curve of S_a for any fuel-air ratio, Mach number and altitude can be obtained by cross-plotting from Figures 3D and 3E.

The magnitudes of S_a were calculated and compared for the combustion efficiencies, $\eta_c = 100\,\%$ and 85 %, based on the heating value of the fuel; and it was found that the S_a for $\eta_c = 85\,\%$ was 95 % of the S_a for $\eta_c = 100\,\%$. This fact could serve to re-define the combustion efficiency; that is, in terms of S_a the new combustion efficiency, η_{S_a} would be 95 % for the instance where 85 % of the heating value of the fuel was actually utilized in combustion (see Figure 3A).

It should be stated here that applying an efficiency factor to the heating value and then entering the chart is not entirely valid, as each Thermodynamic chart of Reference 2 was made up for the full heating value of the particular (1+f) mixture. However, after considerable investigation and various calculations it was concluded that the error thus introduced is negligibly small.

As was explained in the derivation, the magnitude of

$F = A(P + \frac{\rho}{g} V^2)$ is constant from station 2 to station 3 except for flame holder losses. Some interesting relationships can be derived from this equation. When divided by the weight flow the following results:

$$(11) \qquad \frac{F}{\rho V A} = \frac{AP + \frac{\rho}{g} V^2 A}{\rho V A} = \frac{P}{\rho V} + \frac{V}{g} = \frac{RT}{V} + \frac{V}{g}$$

For station 2

$$(11a) \qquad \frac{F_2}{W_a} = \frac{RT_2}{V_2} + \frac{V_2}{g}$$

Thus F_2 is dependent only on T_2 and V_2 and involves no assumption regarding γ. The slope of the line $\frac{F_2}{W_a}$ vs T_2 can be readily seen as $\frac{R}{V_2}$.

This relation presents a very convenient method for obtaining $\frac{F_2}{W_a}$ for different flight Mach numbers and altitudes, but the magnitude of $\frac{F_3}{W_a}$ or $\frac{F_{2'}}{W_a}$, which is less than $\frac{F_2}{W_a}$ by the loss due to the flame holders, is, in general, required. Previously, as given in Reference 6, the loss of pressure due to the flame holders was defined in terms of velocity head, $\rho\frac{V^2}{2g}$, which can be represented as a force $\Delta P \cdot A$. The effect of the change in ρ_2 and V_2 across the flame-holders can be neglected, as calculations prove the error to be very small. Therefore

$$(12) \qquad F_2 - \Delta P \cdot A = F_3$$

or

$$(13) \qquad F_{2'} = F_2 - \frac{n\rho V^2}{2g} = F_3$$

Where n = the number of velocity heads loss. Dividing by the weight flow at station 2, where W_a = weight of air

$$(14) \qquad \frac{F_{2'}}{W_a} = \frac{RT_2}{V_2} + \frac{V_2}{g} - \frac{nV_2}{2g} = \frac{F_3}{W_a}$$

Note that when n = 2

$$(15) \qquad \frac{F_3}{W_a} = \frac{RT_2}{V_2}$$

$\frac{F_2}{W_a}$ was calculated from Equation 11a and has been plotted versus static temperature for a range of V_2's believed practical at the present (see Figure 3). In order to obtain $\frac{F_3}{W_a}$ an appropriate value of $\frac{nV_2}{2g}$ should be subtracted from the $\frac{F_2}{W_a}$ read off the graph, commensurate with what one's knowledge of, or experience with, flame holder losses dictates. The difference between the total and static temperatures at present day practical value of V_2 is negligible, so that the same abscissa can be used for F_2 as for S_a without introducing appreciable error.

Another interesting application of this family of curves (Figure 3) is the instance where sonic velocity exists at the combustion chamber exit. From the equation

$$\frac{F_3}{W_a} = S_a \, \phi(M_3)$$

it can be seen that when

$$\frac{F_3}{W_a} = S_a,$$

$\phi(M_3)$ and thus M_3 equals one. Because $\phi(M_3)$ can never be

less than one, $\frac{F_3}{W_a}$ must always be equal to or greater than S_a. Therefore, if it is required to find the maximum possible V_2; that is, one which produces sonic velocity at station 3 for a given S_a and T_2 (thus fuel-air ratio, Mach number of flight, and altitude) it is necessary only to enter Figure 3 with $F_2 = F_3 = S_a$, neglecting flame-holder losses, and read V_2. Flame-holder losses can be taken into account by adding to F_2 the amount of the loss, thus reading a slightly lower maximum V_2. A more complete discussion related to the maximum velocities possible at the entrance to the combustion chamber is given in Appendix II.

Thus, from Figure 3, F_3 can be found when V_2 and T_2 are known. S_a can be found from Figures 3A-3E for the T_2 and fuel-air ratio used. Then $\phi(M_3)$ can be obtained from $F_3 = S_a \phi(M_3)$ Wa, and M_3 can be found from Figure 4A.

Exit Nozzle

Next, the relation between M_3 and M_5 must be established. This is easily done, as the Mach number at various points in a nozzle can be written as a function of the cross-sectional area, assuming isentropic (no shock) flow.

$$\frac{A_o}{A} = \frac{M}{M_o}\left[\frac{1 + \frac{\gamma-1}{2} M_o^2}{1 + \frac{\gamma-1}{2} M^2}\right]^{\frac{\gamma+1}{2(\gamma-1)}} \qquad (16)$$

where subscript o denotes nozzle inlet conditions. Since the equation is "symmetrical" mathematically, subscript o may also denote nozzle outlet conditions. Thus, M_t being equal to 1, the ratio of the area at the inlet or outlet to the area at the throat may be written

$$(17) \qquad \frac{A_o}{A_t} = \frac{1}{M_o}\left[\frac{1 + \frac{\gamma-1}{2} M_o^2}{\frac{\gamma+1}{2}}\right]^{\frac{\gamma+1}{2(\gamma-1)}}$$

Figure 5 shows a plot of $\phi(M)$ (obtained from Figures 4, and 4A for each Mach number) vs A_o/A_t representing subsonic flow from station 3 to 4 and supersonic flow from station 4 to 5. Three curves were plotted, of which two represent the extreme limits of γ corresponding to the temperatures possible at station 3 and 5, and it can be seen that the effect of γ on the magnitude of $\phi(M_5)$ is not noticeable until a $\phi(M)$ greater than 3 is attained, where the curves separate. In this region it is believed that if the mean value of γ were used the values obtained would be very nearly correct, inasmuch as the maximum possible error in $\phi(M_5)$ due to γ is only 3 %. Using this curve, one need only know $\phi(M_3)$. $\phi(M_5)$ can then be obtained by going first to the subsonic curve, then vertically down to the abscissa, reading off the area ratio A_3/A_t. Then move along the abscissa to the proper A_5/A_t and up to the supersonic curve, then horizontally to the ordinate reading off $\phi(M_5)$. If $A_3 = A_5$, as would probably be true in the practical design, one can move vertically down from the subsonic to the supersonic curve and thence to the ordinate $\phi(M_5)$. It can be seen that the slope of the lower curve is very small at large area ratios, therefore, as will be seen from the equation for C_t, there is little loss in C_t due to making $A_5 = A_2$ at magnitudes of $\phi(M_3)$ greater than

2.5 or 3.0.

This method of finding M_5 assumes a 100 % nozzle efficiency. In order to allow for friction and other losses during expansion the following development is given for nozzle efficiency based on total pressure.

(18) $$\rho_3 V_3 A_3 = \frac{\gamma_3 P_3 M_3 A}{C_3} = \text{a constant}$$

(19) $$\text{Also } C_3 = \frac{C_{s3}}{\left[1 + \frac{\gamma-1}{2} M_3^2\right]^{\frac{1}{2}}} \quad \text{and } P_3 = \frac{P_{T3}}{\left[1 + \frac{\gamma-1}{2} M_3^2\right]^{\frac{1}{2}}}$$

(20) Substituting (19) in (18) and reducing, the following is obtained

$$\frac{\gamma_3 P_{T3} M_3 A_3}{C_{s3}\left[1 + \frac{\gamma-1}{2} M_3^2\right]^{\frac{\gamma_3+1}{2(\gamma_3-1)}}} = \frac{\gamma_5 P_{T5} M_5 A_5}{C_{s5}\left[1 + \frac{\gamma-1}{2} M_5^2\right]^{\frac{\gamma_5+1}{2(\gamma_5-1)}}}$$

Noting that, for an adiabatic process, $C_{s3} = C_{s5}$;

(21) $$\frac{A_3}{A_5} = \frac{P_{T5}}{P_{T3}} \frac{M_5}{M_3} \frac{\gamma_5}{\gamma_3} \frac{\left[1 + \frac{\gamma_3-1}{2} M_3^2\right]^{\frac{\gamma_3+1}{2(\gamma_3-1)}}}{\left[1 + \frac{\gamma_5-1}{2} M_5^2\right]^{\frac{\gamma_5+1}{2(\gamma_5-1)}}}$$

(22) Let $\frac{P_{T5}}{P_{T3}} = \eta_{np}$ and neglect the term $\frac{\gamma_5}{\gamma_3}$ in view of the small effect it has on the magnitude of $\phi(M_5)$.

$$(23)\qquad \frac{A_3}{A_5} = \frac{\frac{1}{M_3}\left[\frac{1+\frac{\gamma_3-1}{2}M_3^2}{\frac{\gamma_3+1}{2}}\right]^{\frac{\gamma_3+1}{2(\gamma_3-1)}}}{\frac{1}{M_5}\left[\frac{1+\frac{\gamma_5-1}{2}M_5^2}{\frac{\gamma_5+1}{2}}\right]^{\frac{\gamma_5+1}{2(\gamma_5-1)}}}$$

$$(24)\qquad \text{Thus } \frac{A_3}{A_5} = \eta_{np}\frac{\left(\frac{A_3}{A_T}\right)_i}{\left(\frac{A_5}{A_T}\right)_i}$$

where subscript i denotes the area ratio corresponding to isentropic compression or expansion.

This is a convenient expression, as the curves for any efficiency can now be plotted directly from the $\eta_n = 100\ \%$ curve. Curves for $\eta_{np} = 90\ \%$ and $80\ \%$ are shown on Figure 5 and the choice of the proper efficiency can be left to the user's judgment.

The nozzle efficiency defined in terms of energy losses, as shown in Reference 6, assumes a value of 95 %. The efficiency based on total pressure was calculated for a wide range of M_3 and P_3 and was found to vary from 80 % to 95 % corresponding to a constant efficiency of 95 % based on energy. This data was plotted against M_3 (see Figure 5A) and seems to show some lack of consistency, however, the indication of the general trend is somewhat significant. Here it might be stated that more information on nozzle

losses and efficiencies under the conditions of flow encountered in a ram-jet would be welcomed.

Thrust Coefficient

The equation used in calculating C_t is developed as follows:

$$(25) \qquad \text{Thrust} = A_5 \left(P_5 + \frac{\rho_5}{g} V_5^2\right) - A_1 \left(P_1 + \frac{\rho_1}{g} V_1^2\right) - P_1 (A_5 - A_1)$$

which is similar to the equation given in Reference 6.

$$T_g = M (V_5 - V_1) + A_5(P_5 - P_1)$$

From Equation 25,

$$T_g = S_{a5}\, \phi(M_5)\, W_a - A_1 P_1 (1 + \gamma M_1^2) - P_1(A_5 - A_1)$$

Then, since

$$C_t = \frac{T_g}{\frac{1}{2} \rho V^2 A} = \frac{T_g}{\frac{1}{2} P M^2 \gamma A}$$

as $S_{a5} = S_{a3}$ the subscripts can be dropped from the S_a term.

$$C_t = 2\left[\frac{S_a \phi(M_5)\, W_a}{P_1 M_1^2 \gamma A_2} - \frac{A_1 P_1 \gamma M_1^2}{P_1 M_1^2 \gamma_1 A_2} - \frac{P_1 A_5}{P M_1^2 \gamma_1 A_2}\right]$$

$$W_a = \rho_1 V_1 A_1 = \frac{P_1 M_1 g \gamma_1 A_1}{C_1}$$

From which

$$(26) \qquad C_T = 2 \frac{A_1}{A_2} \left(\frac{S_a \phi(M_5) \cdot g}{V_1} - 1\right) - \frac{A_5}{A_2} \frac{2}{M_1^2 \gamma}$$

As described before, the combustion chamber efficiency

can be applied to S_a and the product $\eta_{S_a} \times S_a$ actually used in the C_t equation.

Diffuser

Note that Equation 26, is directly affected by diffuser efficiency through the term A_1/A_2 which can be readily determined by a method similar to that given in Reference 6. The diffuser efficiency is still based on energy considerations

$$\eta_D = \frac{h_{2P} - h_o}{h_{2V} - h_o} \tag{27}$$

which is the ratio of the isentropic change in enthalpy from P_o to P_2 through the diffuser to the actual change in enthalpy.

$$h_{2V} = \frac{V_1^2}{2gJ} + h_o - \frac{V_2^2}{2gJ} \tag{28}$$

where subscript 1 denotes conditions at the diffuser entrance and subscript o denotes ambient conditions.

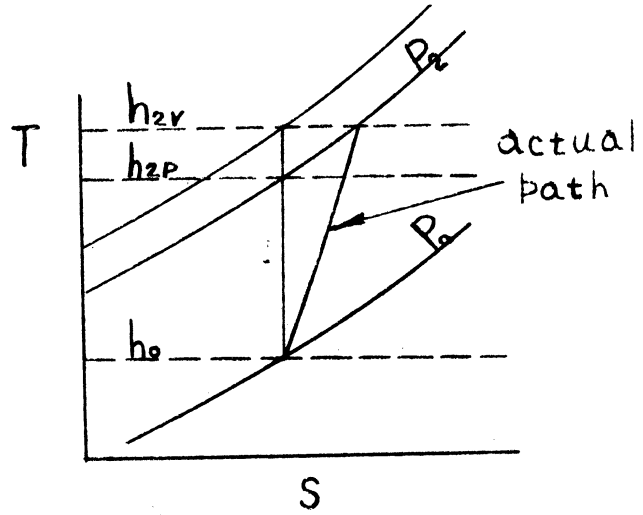

Substituting (28) in (27) and solving for h_{2P} the following is obtained

$$h_{2P} = \frac{\eta_D}{2gJ}(V_1^2 - V_2^2) + h_o \tag{29}$$

where η_D is obtained from Figure 2B. Also from the continuity and state equations, the following results:

$$(a)\quad \rho_1 V_1 A_1 = \rho_2 V_2 A_2$$

$$(b)\quad \frac{P}{\rho} = RT$$

$$(c)\quad P_2 = \frac{P_{r2} P_o}{P_{ro}}$$

and thus

$$(30)\qquad \frac{A_1}{A_2} = \frac{P_{r2}}{P_{ro}} \frac{T_o}{T_2} \frac{V_2}{V_1}$$

where Pr is the Pressure Ratio corresponding to an enthalpy or temperature (see Reference 1) and Pr_2 is the final Pressure Ratio after a non-isentropic change in pressure through the diffuser corresponding to the h_{2P} from Equation 29. The diffuser efficiency is also left undetermined so that it can be chosen to suit the particular problem. (Figure 2B is included in this report as a basis for assumptions).

At this point, it should be clearly understood that the above method also can be applied to a problem involving a fixed design ram-jet. In the fixed design calculations, the area ratio, A_1/A_2, would be known and thus V_2 would be determined by the following:

$$V_2 = \frac{P_{ro} T_2 V_1 A_1}{P_{r2} T_o A_2}$$

Inasmuch as some investigators prefer to define diffuser efficiency on the basis of pressure recovery, the following equation may be used for obtaining V_2 directly;

$$V_2 = \eta_P \frac{P_{ro}}{P_{ri}} \frac{T_2 V_1 A_1}{T_o A_2}$$

where Pr_i is the total pressure ratio (isentropic) and corresponds to h_{2V}. Neglecting V_2 in Equation 28,

$$h_{2V} = \frac{V_1^2}{2gJ} + h_o$$

Figure 2 shows h vs Pr from the Air Tables (Reference 1) and also has tabulated Pr_o, T_o, h_o, and C_o (sonic velocity) for various altitudes within the atmosphere, permitting rapid calculation of ram-jet performance without reference to material other than what is contained in this report.

Some performance figures previously calculated by the method presented in Reference 6 were compared with those obtained for the same conditions by the method presented herein, and the maximum error was found to be 5 %. The S_a term is largely responsible for this discrepancy as it is quite critical. A small error in determining the exact magnitude of S_a for a particular fuel-air ratio and T_2 can cause a greater error in C_t. This also serves to demonstrate the critical nature of the efficiency of combustion, as it directly affects S_a.

BRIEF OUTLINE OF METHOD

(The following is intended as an aid and guide in calculating C_t for any Mach number, fuel-air ratio and altitude).

For given Mach number of flight, fuel-air ratio, and altitude, read the following data from Figure 2; h_o, C_o, T_o, Pr_o, and calculate V_1 from Mach number and C_o. Select a diffuser efficiency (Figure 2B) and an usable V_2 and calculate h_2 from

$$h_{2P} = \frac{\eta_D}{2gJ} (V_1^2 - V_2^2) + h_o$$

From h_2 find Pr_2, using Figure 2 or the Air Tables (Reference 1), then calculate A_1/A_2 from

$$\frac{A_1}{A_2} = \frac{Pr_o T_o V_2}{Pr_o T_o V_1}$$

The A_1/A_2 may be known, as in a fixed design, and the V_2 thus determined by the diffuser efficiency; this is a method of trial and error, as a V_2 must be assumed to calculate h_{2P}, from which Pr_2 is found and thus V_2. However, V_2 is not very critical in computing h_{2P} so that usually not more than one re-calculation is necessary (see Sample Calculation I).

From the T_2 (Figure 2A) and V_2, read $\frac{F_2}{W_a}$ from Figure 3 and subtract $\frac{nV_2^2}{2g}$ for flame holder loss to obtain $\frac{F_3}{W_a}$. Also from one of the following; Figures 3A, 3B, 3C, 3D, or 3E, read the S_a for the fuel-air ratio and T_2. (If considerable

calculation is anticipated for a particular altitude and Mach number or fuel-air ratio, the curve can be obtained by cross-plotting from Figures 3D and 3E.) Calculate $\phi(M_3)$ from

$$\phi(M_3) = \frac{F_3}{W_a S_a}$$

If S_a is greater than $\frac{F_3}{W_a}$, either reduce S_a (the fuel-air ratio), or V_2. (See Sample Calculation III). $\frac{F_3}{W_a}$ must always be equal to or greater than S_a as $\phi(M_3)$ can not be less than 1. Knowing $\phi(M_3)$, $\phi(M_5)$ is obtained from Figure 5 for the nozzle efficiency expected, as indicated on the figure. If the fuel-air ratio is low, at low flight speeds, or at a high altitude, any combination which would produce relatively low temperatures at the combustion chamber exit, one should use the $\phi(M_3)$ and $\phi(M_5)$ curves corresponding to the larger γ and conversely for expected high temperatures. However, the error in $\phi(M_5)$ due to using the mean γ would never be over 1.5 %. Then C_t can be calculated from

$$C_t = \frac{2A_1}{A_2}\left(\frac{\eta_{sa} S_a \phi(M_5)\, g}{V_1} - 1\right) - \frac{A_5}{A_2}\,\frac{2}{\gamma M_1^2}$$

Sample Calculation I

PROBLEM: To find C_t for the following conditions:

$A_1 = A_2 = A_5$

Altitude = 40,000 ft

Flight Mach No. = 3.0

Fuel-Air Ratio = .0333 lb fuel per lb air

(50 % stoichiometric)

$\eta_c = .85$ $(\eta_{S_a} = .95)$

SOLUTION:

1. From Figure 2:
   - $h_o = -1.68$ Btu per lb air
   - $Pr_o = .94$
   - $C_o = 974$; $V_1 = 3C_o = 2922$ ft per sec
   - $T_o = 393^\circ R$

2. From $T_2 = 1085^\circ R$

Figure 2A:

3. From $\eta_D = 79$ %

Figure 2B:

4. Select a V_2 for initial calculation = 400 ft per sec

$$h_{2P} = \frac{\eta_D}{2gJ}(V_1^2 - V_2^2) + h_o = \frac{.79}{50,103}\left[(2922)^2 - (400)^2\right] - 1.68 = 130.4$$

5. From Reference 1:

$$Pr_2 = 20.23$$

6. $$V_2 = \frac{Pr_o T_2 V_1 A_1}{Pr_2 T_o A_2} = \frac{.94 \times 1085 \times 2922}{20.23 \times 393 \times 1} = 374.9$$

7. Re-calculating $h_{2P} = \frac{.79}{50,103}\left[(2922)^2 - (370)^2\right] - 1.68 =$

$$= 130.9$$

From Reference 1, $Pr_2 = 20.39$

$$V_2 = \frac{.94 \times 1085 \times 2922}{20.39 \times 393} = 371.9 \text{ ft per sec}$$

8. From Figure 3 or calculate

$$\frac{F_3}{W_a} = \frac{RT_2}{V_2} + \frac{V_2}{g} - \frac{nV_2}{2g}$$

Letting n = 1,

$$\frac{F_3}{W_a} = 170 - \frac{371.9}{64.4} = 164.2$$

9. From Figure 3D: $S_a = 137$

10. $\eta_{S_a} S_a = .95 \times 137 = 130.15$

11. $\phi(M_3) = \frac{164.24}{130.15} = 1.262$

12. From Figure 5 $\phi(M_5) = 1.05$ for $\eta_{np} = 88\ \%$

13. $$C_t = \frac{2A_1}{A2}\left[\frac{\eta_{S_a} S_a \phi(M_5) g}{V_1} - 1\right] - \frac{A_5}{A_2}\frac{2}{\gamma M_1^2}$$

$$= 2\left[\frac{(130.15)(1.05)32.2}{2922} - 1\right] - \frac{2}{1.4(3)^2}$$

$\boxed{C_t = .85}$ for $A_1 = A_2$ and 1:30 fuel-air ratio

Sample Calculation II

PROBLEM: To find C_t for the following conditions:

Altitude = 20,000 ft

Flight Mach No. = 4.0

V_2 = 200 ft per sec

Fuel-Air Ratio = .0665 lbs fuel per lb air

(100 % stoichiometric)

$\eta_c = 85\%$ ($\eta_{S_a} = 95\%$)

SOLUTION:

1. From Figure 2:
   - $h_o = 11.24$ Btu per lb air
   - $Pr_o = 1.474$
   - $C_o = 1037.5$; $V_1 = 4C_o = 4150.0$ ft per sec
   - $T_o = 446.8^\circ R$

2. From Figure 2A: $T_2 = 1790^\circ R$

3. From Figure 2B: $\eta_D = .70\ \%$

4. $$h_{2P} = \frac{\eta_D}{2gJ}(V_1^2 - V_2^2) + h_o = \frac{.70}{50,103}(4150^2 - 200^2)$$
   $$+ 11.24 = 251.3 \text{ Btu per lb}$$

5. From Reference 1, (or Figure 2)
   $$Pr_2 = 92.23 \text{ (corresponds to } h_{2P} = 251.3)$$

6. $$\frac{A_1}{A_2} = \frac{Pr_2}{Pr_o}\frac{T_o}{T_2}\frac{V_2}{V_1} = \frac{92.23}{1.474}\frac{200}{4150}\frac{446.8}{1790} = .753$$

7. From Figure 3

$$\frac{F_2}{W_a} = 484$$

Flame holder loss, $(n = 2) = \frac{2V_2}{2g} = \frac{400}{64.4} = 6.21$ thus

$$\frac{F_3}{W_a} = 484 - 6.21 = 477.79$$

8. From Figure 3A

$$S_a = 177.5$$

9. $F_3 = S_a \, \phi(M_3) \, W_a$ $\qquad \phi(M_3) = \frac{477.78}{177.5} = 2.692$

10. From Figure 5, taking $A_5 = A_3$

$\phi(M_5) = 1.21$ for $\eta_{np} = 80$ % (low according to Figure 5A)

11. $$C_t = \frac{2A_1}{A_2}\left(\frac{S_a \phi(M_5) g}{V_1} - 1\right) - \frac{2A_5}{A_2 \gamma M_1^2} =$$

$$= 2(.753)\left[\frac{177.5 \times 1.21 \times 32.2}{4150} - 1\right] - \frac{2}{1.4(4)^2}$$

$$\boxed{C_t = .914}$$

Sample Calculation III

PROBLEM: To calculate C_t for the following conditions:

Altitude = Sea Level

Flight Mach No. = 2.0

V_2 = 350 ft per sec

Fuel-Air Ratio = .0605 (Lean) (91 % stoichiometric)
lb fuel per lb air

η_c = .85 (η_{S_a} = .95)

SOLUTION:

1. From Figure 2:
   - h_o = 28.56 Btu per lb air
   - Pr_o = 2.49
   - C_o = 1117.50; $V_1 = 2C_o$ = 2235 ft per sec
   - T_o = 519.0°R

2. From Figure 2A: T_2 = 920°R

3. From Figure 2B: η_D = .85 %

4. $$h_{2P} = \frac{\eta_D}{2gJ}(V_1^2 - V_2^2) + h_o = \frac{.85}{50{,}103}(2235^2 - 350^2) +$$
$$+ 28.56 = 111.22 \text{ Btu per lb air}$$

5. From Reference 1:

$$Pr_2 = 14.82$$

6. $$\frac{A_1}{A_2} = \frac{Pr_2}{Pr_o}\frac{T_o}{T_2}\frac{V_2}{V_1} = \frac{14.82}{2.49}\frac{519}{920}\frac{350}{2235} = .525$$

7. From Figure 3 or calculate

$$\frac{F_3}{W_a} = \frac{RT_2}{V_2} = \frac{53.34 \times 920}{350} = 140.2$$

(for two velocity heads, loss at flame holders $n = 2\left(\frac{\eta V_{2'}}{2g}\right)$)

8. From Figure 3B $S_a = 160$, which is larger than F_3, thus $\phi(M_3) < 1$; as this is impossible either reduce S_a or decrease V_2 and re-calculate.

9. Reduce S_a to 140; i.e., make mixture more lean -

10. $$\phi(M_3) = \frac{F_3}{S_a W_a} = 1 \quad \phi(M_5) = 1$$

11. $$C_t = \frac{2A_1}{A_2}\left[\frac{S_a \phi(M_5) g}{V_1} - 1\right] - \frac{2A_5}{A_2 \gamma M_1^2} =$$

$$= 2(.525)\left[\frac{140.2 \times 32.2}{2235} - 1\right] - \frac{1}{2(1.4)}$$

$$\boxed{C_t = .714}$$

REFERENCES

1. J. H. Keenan and J. Kaye, "Thermodynamic Properties of Air." First Edition. New York, John Wiley and Sons, Inc. (1945)
2. R. L. Hershey, J. E. Eberhart, and H. C. Hottel, "Thermodynamic Properties of the Working Fluid in Internal Combustion Engines." New York, S.A.E. Journal, Vol. 39, No. 4, Pages 409-424 (October 1936).
3. JHU/APL, CM-1. "Momentum of Combustion", Philip Rudnick (6 January 1945).
4. JHU/APL, CM-236. "Ram-jet Thrust Coefficients and Specific Impulse." A. C. Beer. (April 1946).
5. JHU/APL Bumble-Bee Report No. 32. "Analysis of Internal Flow in Ram-jets." Thomas Davis and J. R. Sellars. (March 1946)
6. University of Michigan External Memorandum No. 1, "An Analysis of the Performance Characteristics of the Ram-Jet Engine." E. T. Vincent. (25 January 1947).
7. NACA Tech. Note No. 1026. "Charts of Thermodynamic Properties of Fluids Encountered in Calculations of Internal Combustion Engine Cycles." H. C. Hottel and G. C. Williams. (M.I.T.)

Appendix I

Validity of method presented in UMM-1 (see Reference 6) for special cases.

This portion of the report is the result of an investigation which had as its objective the presentation of evidence that the method presented in Reference 6 accounts for the particular condition of flow where a Mach number of one exists at the combustion chamber exit and that no solution could be obtained if a higher Mach number would be required at this station. During the course of this investigation it was found that the method of solution given in Reference 6 gave two solutions at low flight velocities for the velocity at the end of the combustion chamber, one being supersonic and of no practical significance, while only one solution could be obtained at higher flight velocities. This was somewhat unexpected and warranted further investigation even though the supersonic solution was only of academic interest. The work that followed led to the development of the method of calculation given in the main body of this report and the explanation given there regarding the presence of two solutions for the flow conditions at the end of the combustion chamber is believed adequate. The following consists of a detailed description of the method of solution as given in Reference 6 and some representative graphical evidence which shows that the method is valid for the instances where sonic velocity exists at the combustion chamber exit and that the

method would give no solution if velocities greater than sonic were required.

Figures I and IA show the results of a series of calculations to determine the exit conditions from a cylindrical combustion chamber for various inlet air velocities (V_2). See Figure A for the location of various sections referred to as station 2, 3, etc. The method is by trial and error; i.e., a value is assumed for V_3, and by satisfying the energy, force-momentum and state equations, trial values of P_3, ρ_3, and T_3 are determined. Then, satisfying the continuity of mass flow equation determines if the proper V_3 was initially chosen. Figure 1 is a plot of the trial solutions for various combustion chamber inlet velocities at a flight Mach number of 1.75 at 40,000 feet with a fuel-air ratio of .0665. This diagram plots the initially assumed velocity at station 3 against the final velocity determined by the continuity equation, after having satisfied the energy, force-momentum, and state equations. It follows that the assumed V_3 which gives a calculated V_3 of the same magnitude is the correct solution for the flow at the conditions of the problem. Thus the curves of Figure I and IA show the calculated V_3 plotted against the assumed V_3 for various values of combustion chamber inlet velocity (V_2). The straight line in both figures having a slope of 1 is necessarily the locus of all solutions for V_3; i.e., the assumed velocity equals the calculated velocity. Therefore, the intersections of each curve with the straight line are V_3 solutions for the

particular conditions represented by the curve.

A point worth noting is the small difference in the value of V_2 necessary to give two widely spaced solutions, or no solution. For instance, in Figure 1 the V_3 solutions for a V_2 or 205 ft per sec are 2305 ft per sec and 3105 ft per sec while for a $V_2 > 207$ no solution is obtained. Thus the method under discussion can be employed with a high degree of a accuracy to obtain the V_2 that produces choking, but only after considerable calculation and work involving the Thermodynamic Charts. (Reference 2).

In the instance where no solution appeared ($V_2 = 208$ ft per sec in Figure 1) the heat addition (fuel-air ratio) was decreased and a solution proved to be possible. Thus it is established that the method under discussion would offer no solution if conditions in the combustion chamber entrance were such that for a given heat addition, velocities greater than the local sonic velocity would be required at the end of the combustion chamber. Consequently, it is concluded that the data presented in Reference 6 does represent possible solutions to the problem as there outlined despite some differences with the conclusions derived by other investigators.

Appendix II

Probable Magnitude of the Air Velocity at the Entrance to the Combustion Chamber.

It is of interest to note from Figure 3 that at those values of T_2 corresponding to high Mach numbers (5,6) the upper limits of the combustion chamber entrance velocity, V_2, established by the fundamental equations governing flow in a duct are of the order 700-1000 ft per sec for a maximum S_a (approximately stoichiometric fuel-air ratio). As the fuel-air mixture is made more lean, reducing S_a, the maximum V_2 increases even more. However, the applications of a particular ram-jet design that would use these excessively high velocities are believed very limited, for the following reasons:

At low Mach numbers, say those less than 2.8 to 3.0, the maximum C_t is obtained by using maximum S_a with the corresponding maximum V_2 such that sonic velocity exists at the combustion chamber exit; i.e., no nozzle required - open tail exhaust. At higher Mach numbers the ram-jet configuration corresponding to maximum C_t ($A_1 = A_2$) serves to limit V_2. Figure 6 shows how this maximum V_2 varies with Mach number at various fuel-air ratios, and also how it varies for $A_1 = A_2$.

At low Mach numbers the ratio of the diffuser inlet area to the combustion chamber area, A_1/A_2, would necessarily be less than unity, and as the Mach number increases

at a constant altitude, for example, the diffuser inlet, A_1, would be made larger, thus increasing V_2, keeping F_3 equal to S_a, and therefore, V_3 equal to local sonic velocity, until A_1 equals A_2. On Figure 6 this would mean moving along the S. L. - .0665 fuel-air ratio curve to its intersection with the S. L. curve of "V_2 for $A_1 = A_2$". At this point the best C_t possible for that particular altitude of flight and fuel-air ratio will be attained (see Figure 7). As the ram-jet accelerates further to higher Mach numbers, A_1 should be kept equal to A_2 and a tail nozzle should be used, whose area ratio varies as required by M_3. If A_1 is made greater than A_2, the C_t (referred to the maximum frontal area) will decrease, because this will cause an increase in V_2 and, as was established in Reference 6, the thrust per lb of air decreases with an increase in V_2. It also follows that if S_a is reduced at constant flight conditions (by reducing fuel-air ratio) the diffuser inlet area A_1 should be opened up increasing V_2. Thus, V_3 is kept equal to the local sonic velocity until A_1 equals A_2, at which point further reduction in S_a would necessitate a nozzle. Figure 6 shows that for the .0665 fuel-air ratio, which would be used to obtain the greatest C_t, the maximum V_2 is approximately 450 ft per sec (intersection of S. L. .0665 curve with S. L. $A_1 = A_2$ curve). It also can be seen that the diffuser efficiency affects this peak, causing an increase in the maximum V_2 for a less efficient diffuser.

Rough calculations seem to indicate that the maximum specific impulse, Ig, occurs at a fuel-air ratio of approxi-

mately .04; for this reason, the curve corresponding to a fuel-air ratio of .04 was also sketched on Figure 6, and the maximum V_2 for this curve appears to be 480 ft per sec.

Thus, the maximum V_2 that would ever be considered in designs where either maximum C_t or maximum specific impulse, Ig, (reduced S_a) were the primary objectives would be something less than 500 ft per sec, unless these assumed diffuser efficiencies prove to be too optimistic.

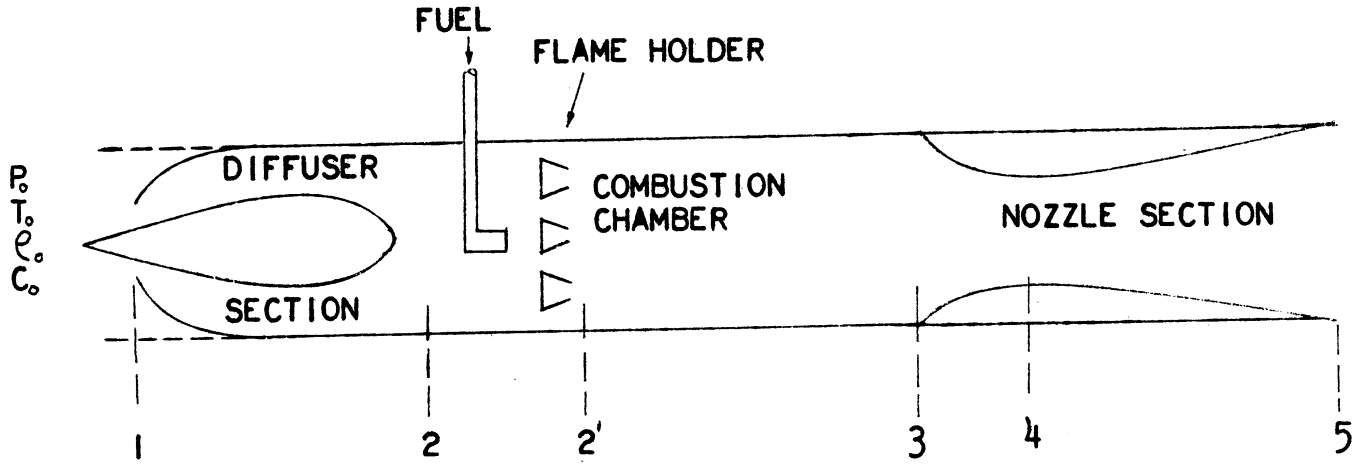

FIG. A RAM-JET STATION DESIGNATION (REFERRED TO AS STN. 2, 3 ETC.)

Figure No. 1

SOLUTION FOR VELOCITY AT STN. 3 (RAM-JET)

*Marks solution

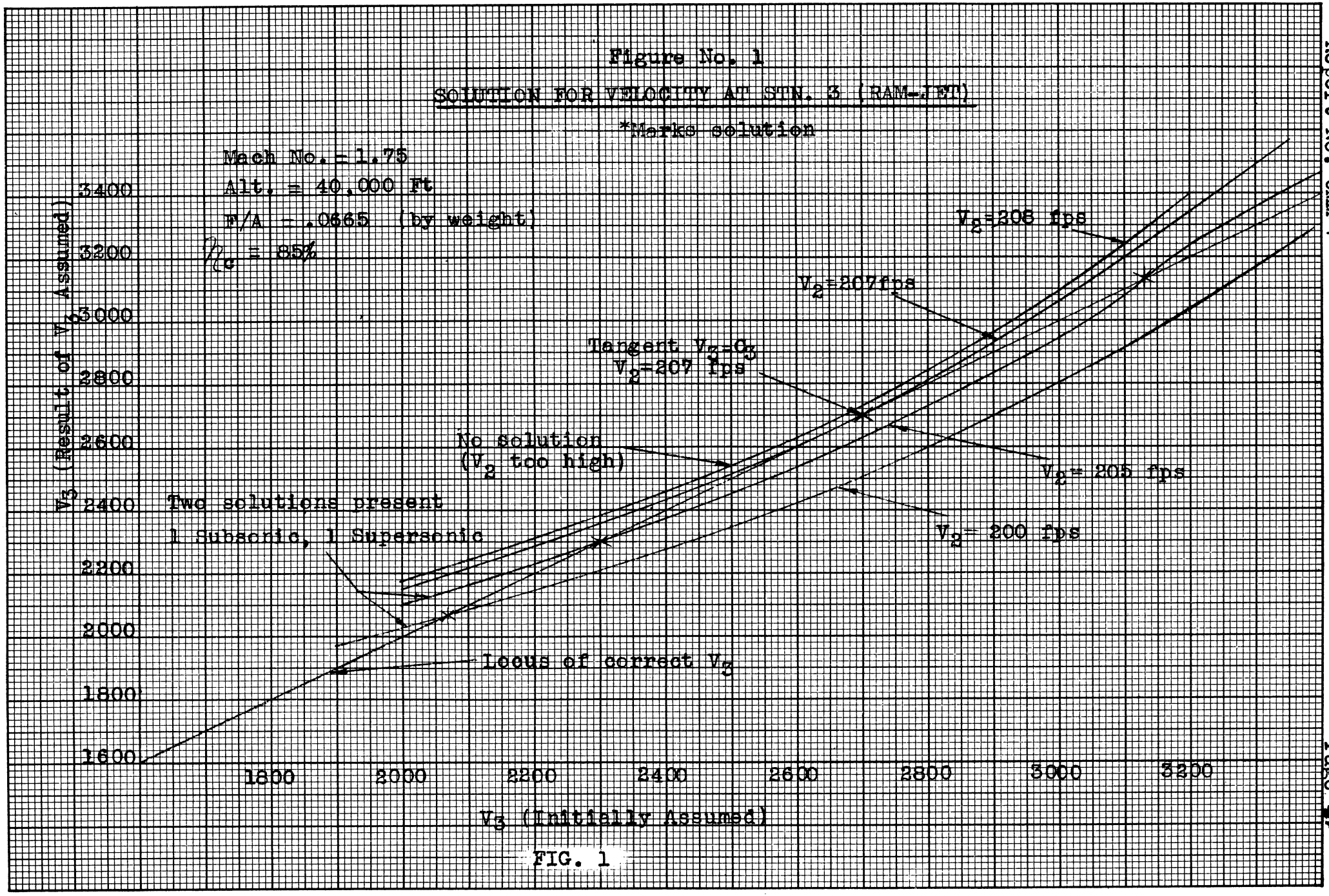

FIG. 1

Figure No. 1A

SOLUTION FOR V_3 (RAM-JET)

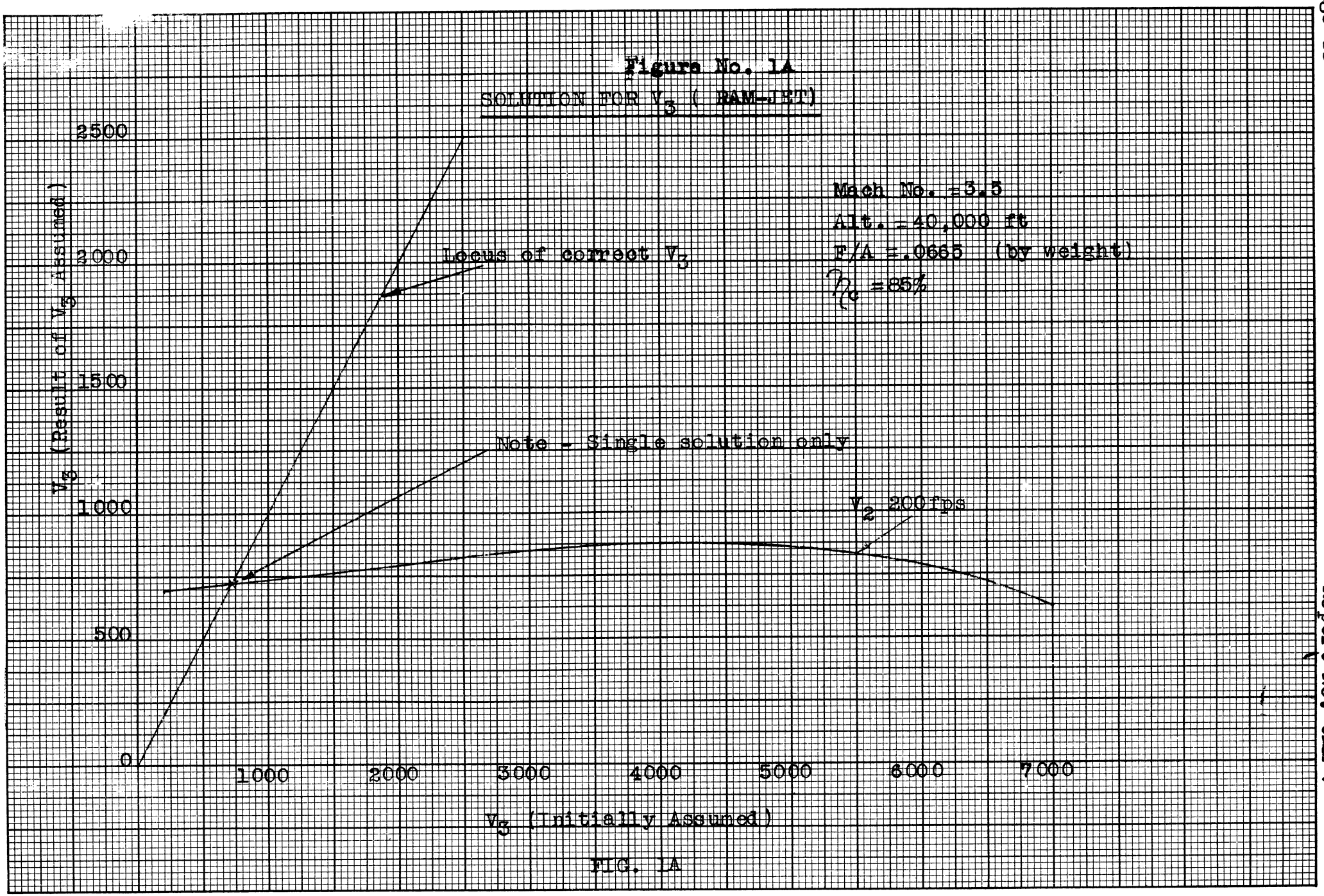

FIG. 1A

Figure No. 2

CHART FOR USE IN CALCULATING A_1/A_0

M_2 vs Pr_{t2}
(Data from Ref.1)

M_2 - Exhaust Mach No.

Pr_2 - Pressure Ratio

Altitude h_0	Isothermal	Pressure Ratio Pr_0	Sonic Velocity C_0	Temperature °R T_0
40,000	Assumed constant above 36,332 ft			
36,332	-1.68	.94	974	393
30,000	2.82	1.108	996	412
25,000	7.14	1.236	1016	429.8
20,000	11.24	1.474	1037.6	436.8
15,000	15.78	1.70	1058.5	455.5
10,000	19.98	1.938	1078.0	455.4
5,000	24.25	2.203	1098.0	501.2
S. L.	28.56	2.49	1117.5	519.0

*Table 1. Based on "NACA Std. Temp." and the "Air Tables" - see Ref.1)

$$h_2 = \frac{2g_0}{2gJ}(V_1^2 - V_2^2) + h_0$$

$$A_1/A_0 = \frac{Pr_{t2}}{Pr_0}\frac{V_2}{V_0}\frac{T_0}{T_2}$$

Pr_2 - Pressure Ratio

Fig. 2

PRINTED IN U.S.A.

EUGENE DIETZGEN CO. NO. 346 D

Figure No. 2A

TOTAL TEMPERATURE VS FLIGHT MACH NO.

Data from Air Tables (see Ref. 1)

Temperatures can be read as total temperatures, or as static temperat ures for local velocities up to 500fps.

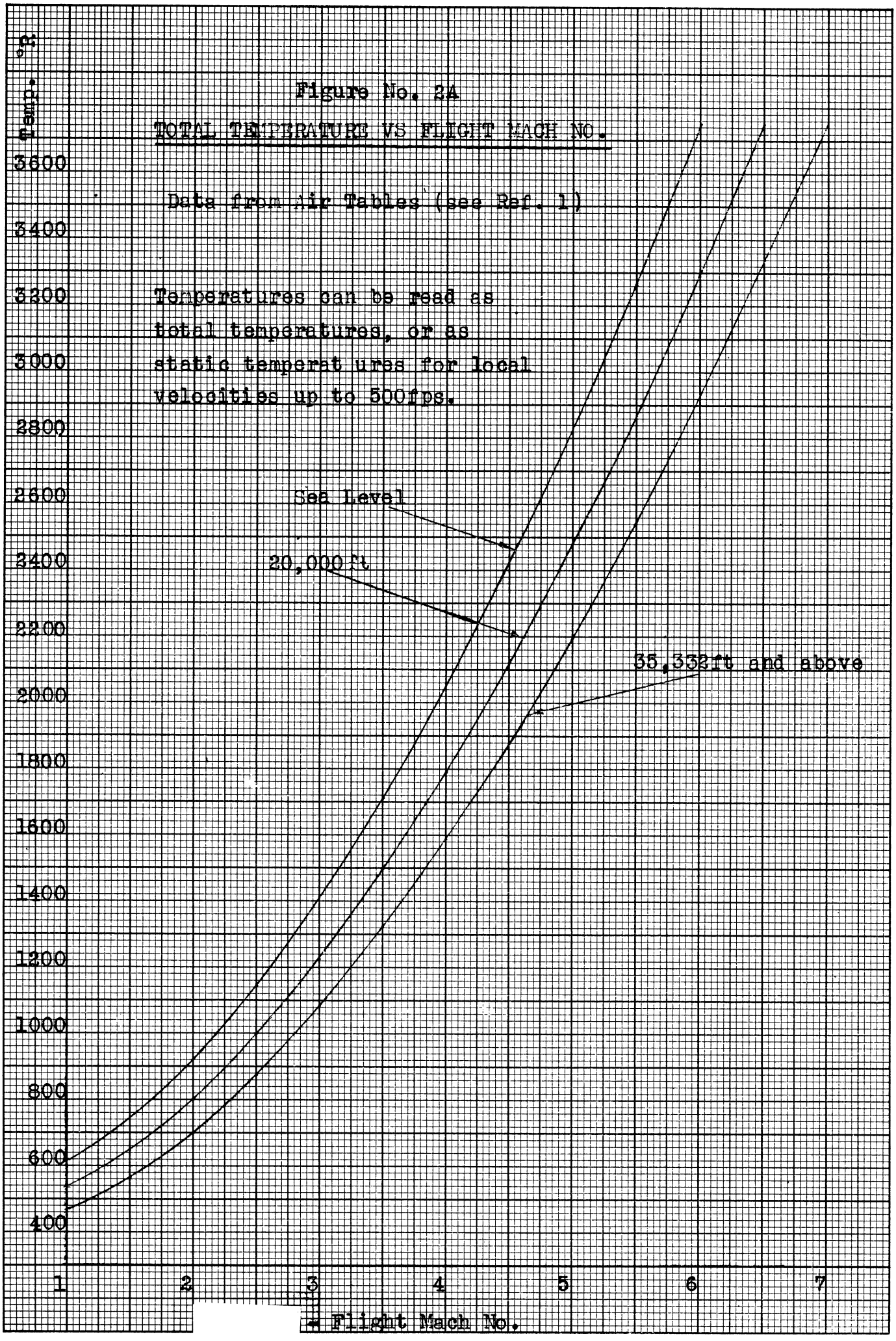

Figure No. 2B
DIFFUSER EFFICIENCY VS MACH NUMBER
(Based on current estimates)
Diffuser Efficiency - η_D
.5
.6
.7
.8
.9
1.0
1
2
3
4
5
6
Flight Mach Number

FIG. 2B

Figure No. 3
SPECIFIC STREAM THRUST - F_2/W_a VS T_2 FOR VARIOUS V_2's
$F = A(p + \rho V^2)$
$F_2/W_a = \frac{RT_2}{g} + \frac{V_2}{g}$
V_2 = 140
160
180 fps
200
225
250
275
300
325
350
375
400
500
Specific Stream Thrust - F_2/W_a (lbs per lb air per sec)
1100
1000
900
800
700
600
500
400
300
200
100
0
400
800
1200
1600
2000
2400
2800
3200
Temperature at entrance to combustion chamber- T_2 °R

FIG. 3

Figure No. 34
HEAT RELEASE - S_e vs T_2
Normal fuel-air ratio (.0665 lb fuel per lb air)
(Stoichiometric)
$\eta_{ae} = 100\%$
$\eta_e = 95\%$
$\eta_{ae} = 95\%$
$\eta_e = 80\%$
S_e
200
180
160
140
120
100
80
60
400
800
1200
1600
2000
2400
2800
3200
Temperature at entrance to combustion chamber - T_2 - °R.

FIG. 34

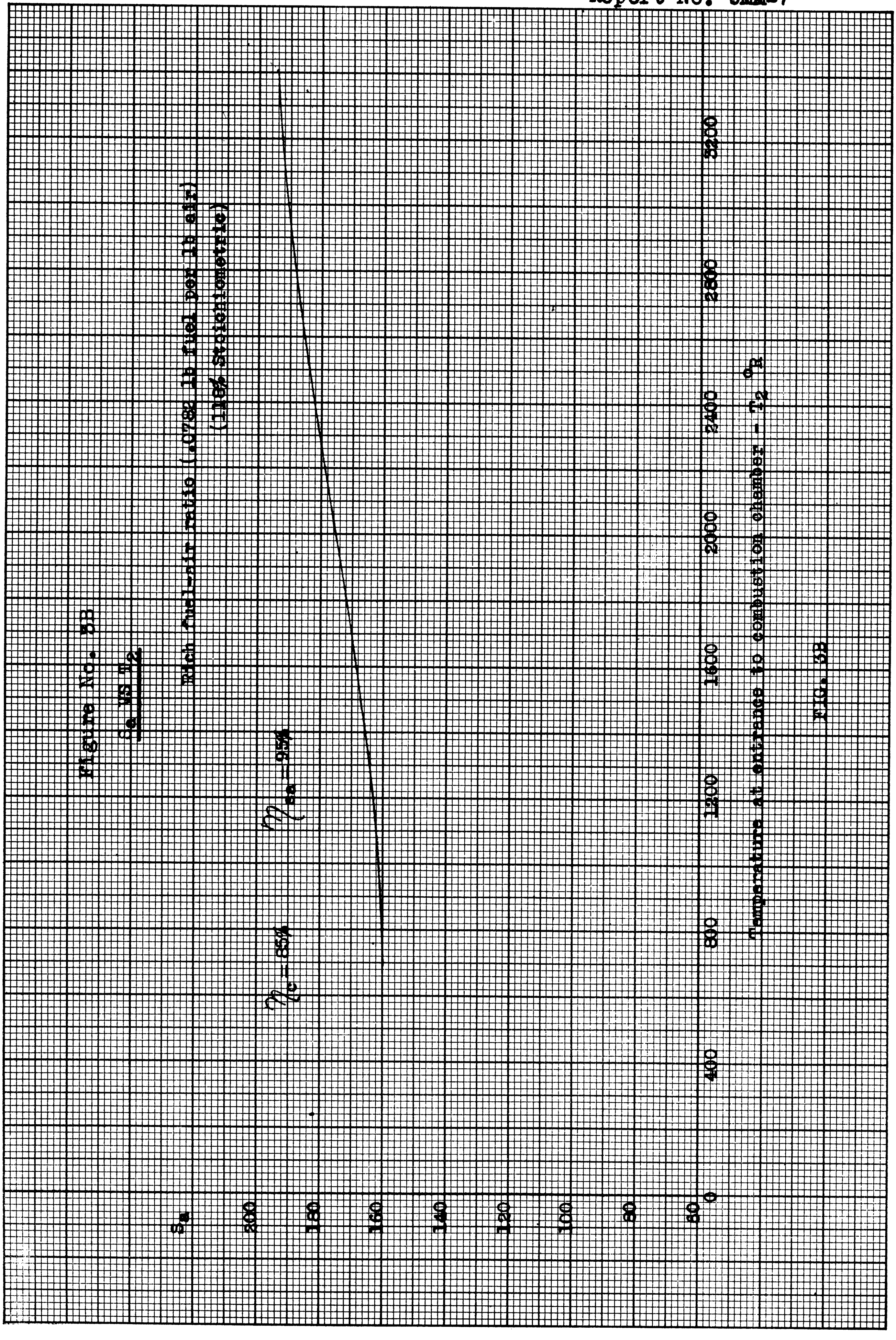
Figure No. 3B
Sa VS T2
Rich fuel-air ratio (.0782 lb fuel per lb air)
(110% Stoichiometric)
ηc = 85%
ηsa = 95%
Sa
200
180
160
140
120
100
80
60
0
400
800
1200
1600
2000
2400
2800
3200
Temperature at entrance to combustion chamber - T2 °R

FIG. 3B

Figure No. 50
Sea FS 42
Lean fuel-air ratio (.0505 lb fuel per lb air)
(91% Stoichiometric)
$\eta_c = 85\%$, $\eta_{ac} = 95\%$
T_3 - Temperature at entrance to combustion chamber - °R
3200
2800
2400
2000
1800
1600
1400
1200
1000
800
600
400
0
200
180
160
140
120
100
80
60

FIG. 50

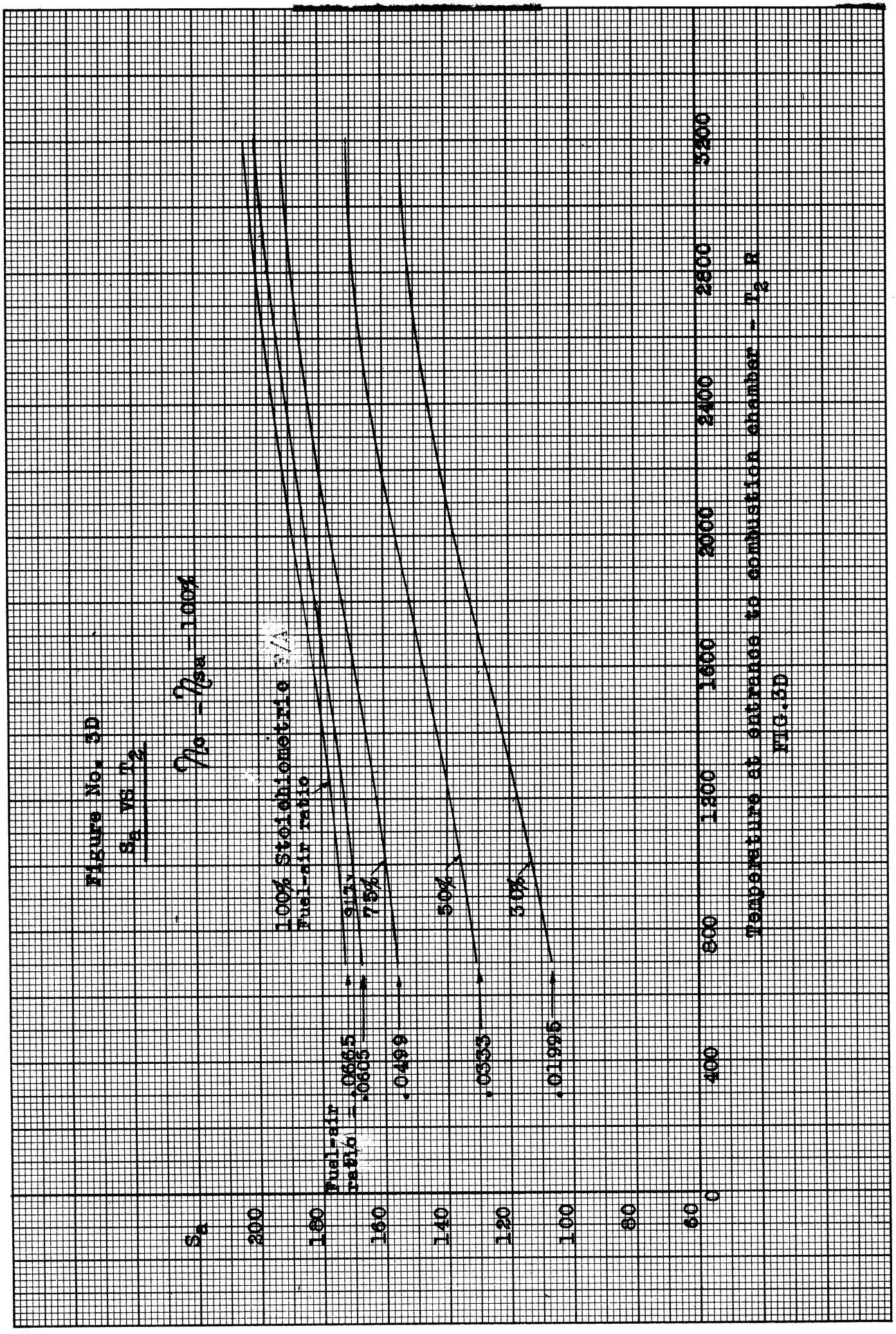
Figure No. 3D
S_a vs T_2
$\eta_o = \eta_{sa} = 100\%$
100% Stoichiometric Fuel-air ratio
91%
75%
50%
30%
.0365
.0405
.0490
.0535
.0595
Fuel-air ratio
S_a
200
180
160
140
120
100
80
60
0
400
800
1200
1600
2000
2400
2800
3200
Temperature at entrance to combustion chamber - °R

FIG.3D

Figure No. 55
S_e vs FUEL-AIR RATIO
(Weight Ratio)
$\Omega_o = \Omega_{oa} = 100\%$
T_2 = 2358 R
2271 R
1329 R
1703 R
S_e
200
180
160
140
120
100
80
60
0
.01
.02
.03
.04
.05
.06
.07
.08
Fuel-Air Ratio
FIG. 55

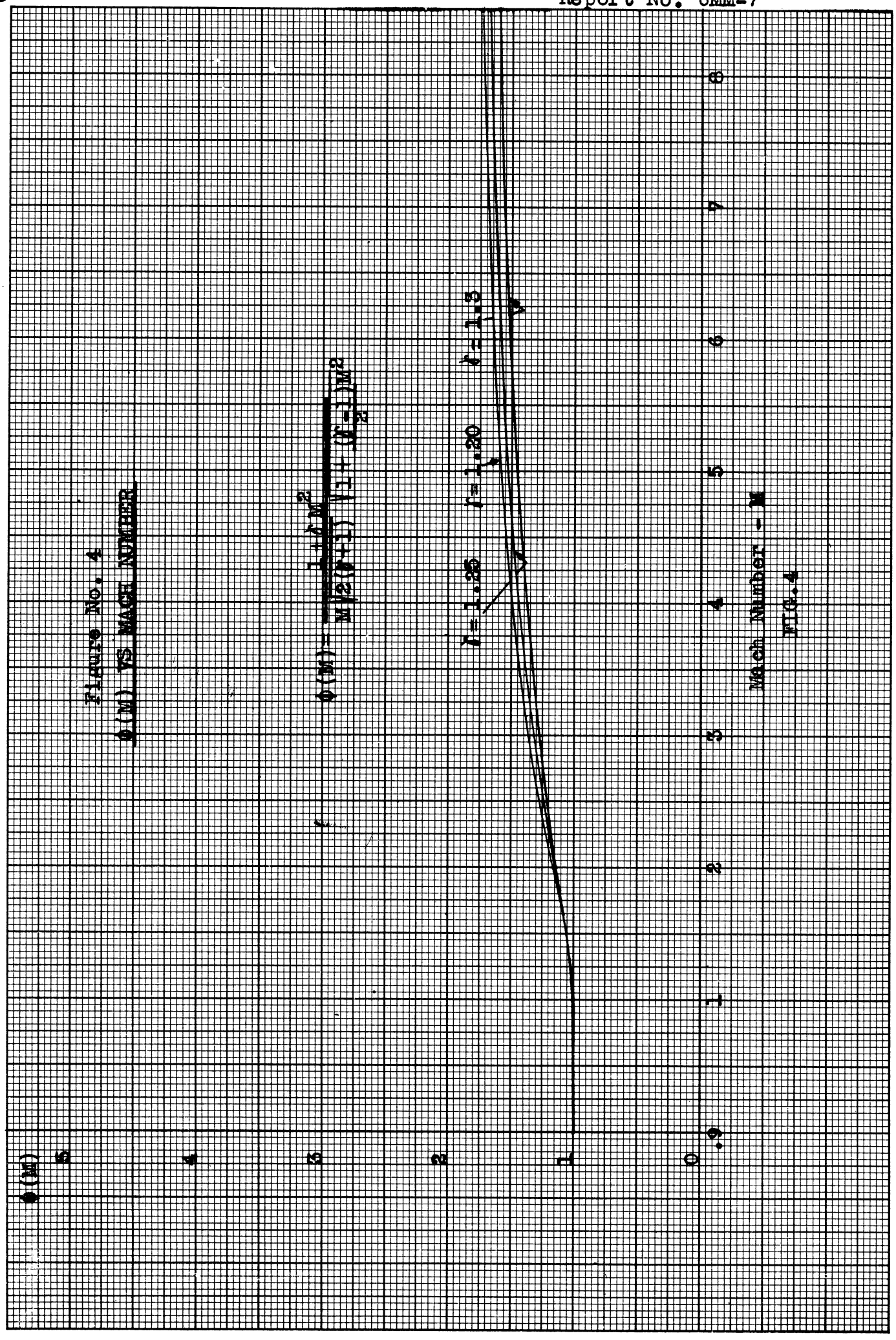
Φ(M) VS MACH NUMBER
Figure No. 4
Φ(M)
Mach Number - M
FIG.4
γ = 1.4
γ = 1.3
γ = 1.2
γ = 1.1
Φ(M) = √((γ+1)/2)^((γ+1)/(γ-1)) M^2 / (1 + ((γ-1)/2) M^2)^((γ+1)/(γ-1))

Figure No. 4A
Φ(M) VS MACH NUMBER
$\Phi(M) = \frac{1+\gamma M^2}{M^2(\gamma+1)}\sqrt{\frac{(\gamma+1)M^2}{2+(\gamma-1)M^2}}$
$\gamma = 1.135$
$\gamma = 1.225$
$\gamma = 1.5$
Φ(M)
5
4
3
2
1
0
.9
.8
.7
.6
.5
.4
.3
.2
.1
Mach Number - M
FIG. 4A

Figure No. 4B
Φ(M) VS MACH NUMBER
Φ(M) = √(M²-1)
(Asymptote)
Mach Number M
FIG.4B
Φ(M)
0
1.0
2
3
4
5
6
7
8
9
10

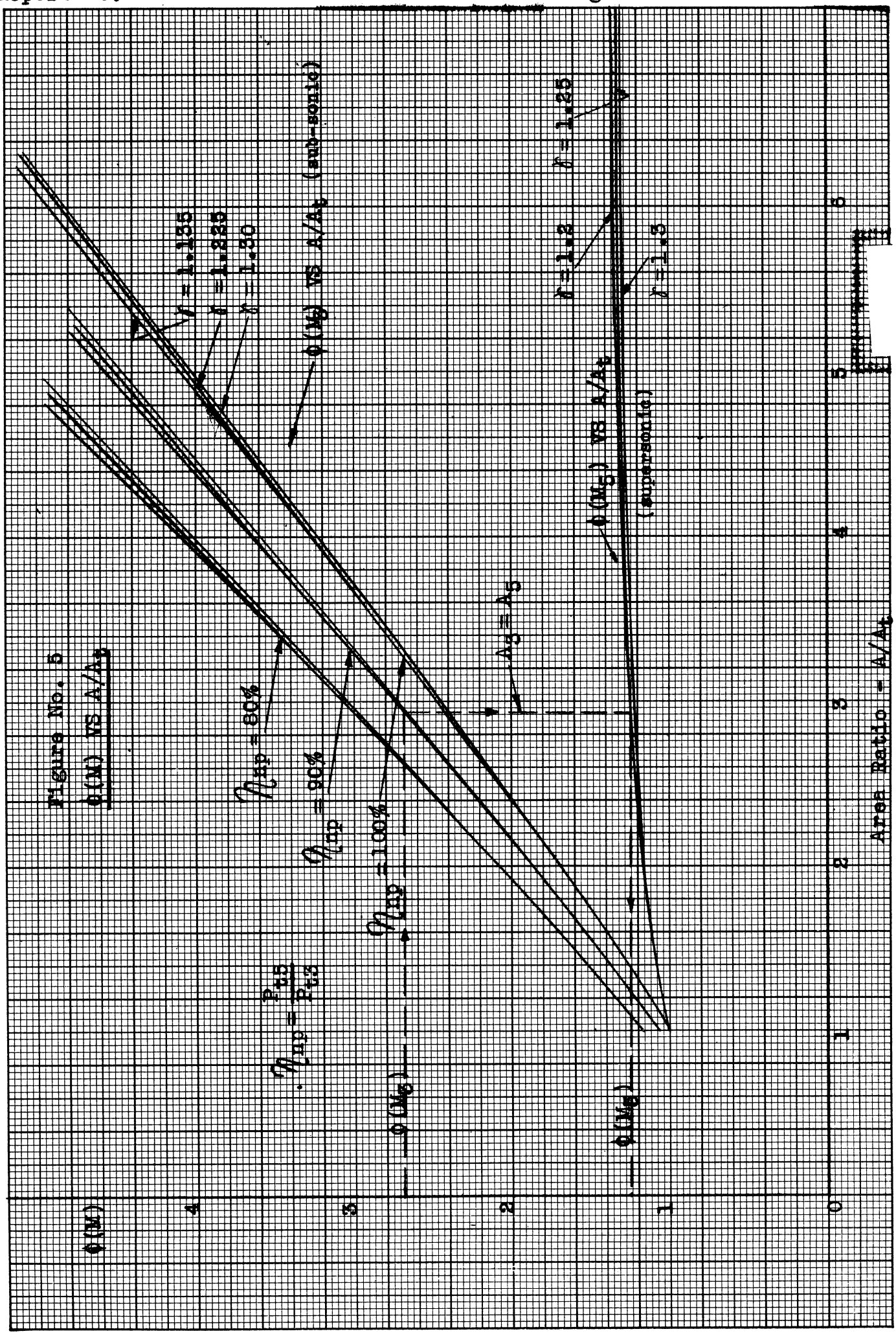
Figure No. 5
Φ(M) VS A/A*
Φ(M)
Area Ratio - A/A*
γ = 1.135
γ = 1.225
γ = 1.30
Φ(M) VS A/A* (sub-sonic)
Φ(M5) VS A/A* (supersonic)
γ = 1.25
γ = 1.2
γ = 1.3
A5 = A5
ηnp = 80%
ηnp = 90%
ηnp = 100%
p = 5
p = 3
Φ(M5)
Φ(M5)

Figure No. 5A

THEORETICAL TOTAL PRESSURE RECOVERY FOR A CONSTANT NOZZLE EFFICIENCY BASED ON ENERGY

(η_{cp} VS M_3)

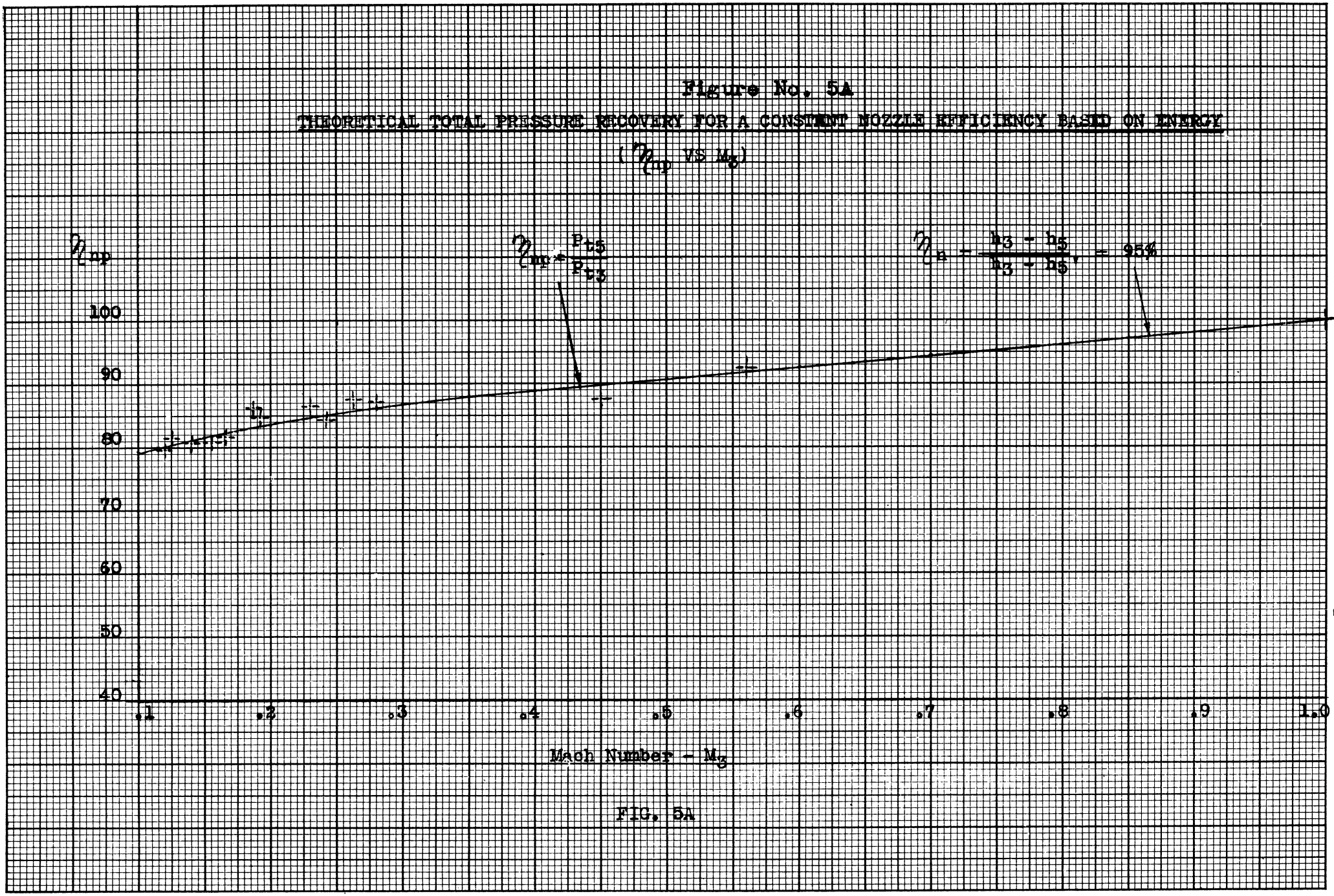

FIG. 5A

Velocity at the entrance to the combustion chamber - V_2
ft per sec
800
700
600
500
400
300
200
100
0
1
2
3
4
5
6
7
FLIGHT MACH NUMBER M_1
η_D From Fig. 2B
$\eta_D = 100\%$
V_2 For $V_3 = C_3$ (No nozzle)
$\eta_c = 80\%$ and two velocity heads lost at flame-holders
V_2 For $A_1 = A_2$
MAXIMUM V_2 FOR $A_1 = A_2$ AND VARIOUS FUEL-AIR RATIOS
FIGURE No. 6
FIG. 6

Figure No. 7

THRUST COEFFICIENT VS FLIGHT MACH NUMBER

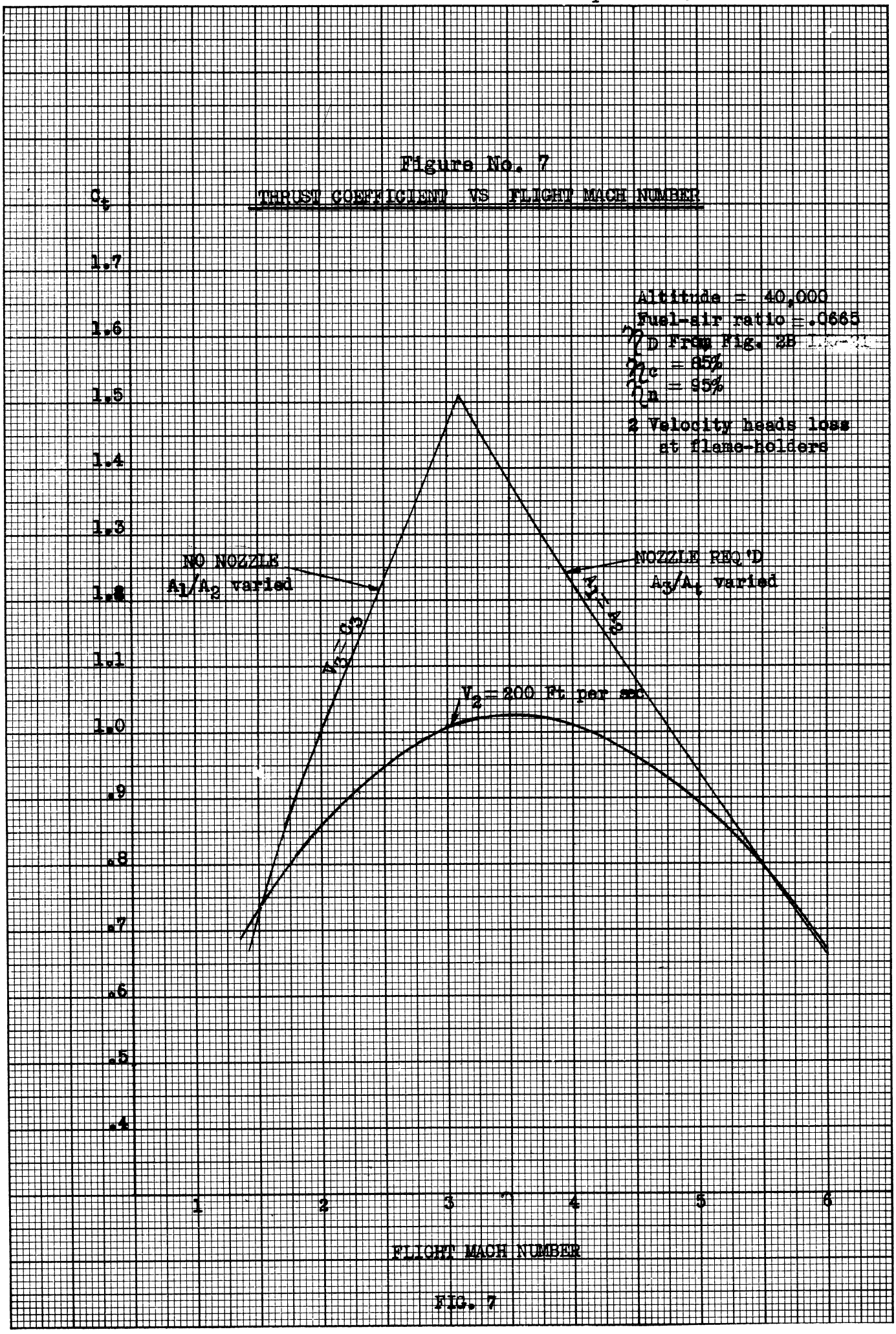

FIG. 7